Comparison of Methods for Estimating Nearshore Shear Wave Variance*

T. JAMES NOYES AND R. T. GUZA

Center for Coastal Studies, Scripps Institution of Oceanography, La Jolla, California

STEVE ELGAR

Woods Hole Oceanographic Institution, Woods Hole, Massachusetts

T. H. C. HERBERS

Naval Postgraduate School, Monterey, California

(Manuscript received 12 January 2001, in final form 13 June 2001)

ABSTRACT

Shear waves (instabilities of the breaking wave–driven mean alongshore current) and gravity waves both contribute substantial velocity fluctuations to nearshore infragravity motions (periods of a few minutes). Three existing methods of estimating the shear wave contribution to the infragravity velocity variance are compared using extensive field observations. The iterative maximum likelihood estimator (IMLE) and the direct estimator (DE) methods use an alongshore array of current meters, and ascribe all the velocity variance at non–gravity wavenumbers to shear waves. The ratio (R) method uses a collocated pressure gauge and current meter, and assumes that shear wave pressure fluctuations are small, and that the kinetic and potential energies of gravity waves are equal. The shear wave velocity variance $\langle q_{sw}^2 \rangle$ is estimated from the relative magnitudes of the total (shear plus gravity wave) pressure and velocity variances. Estimates of root-mean-square shear wave velocity fluctuations $\sqrt{\langle q_{sw}^2 \rangle}$ from all three methods are generally in good agreement (correlations > 0.96), supporting the validity of their underlying assumptions. When $\sqrt{\langle q_{sw}^2 \rangle}$ is greater than a few centimeters per second, IMLE and DE estimates of $\sqrt{\langle q_{sw}^2 \rangle}$ differ by less than 10%. The R estimates of $\sqrt{\langle q_{sw}^2 \rangle}$ are usually higher than the IMLE and DE estimates, and on average the R method attributes 15% more of the total horizontal velocity variance to shear waves than is attributed by the IMLE method. When mean currents and shear waves are weak, all three estimators are noisy and biased high.

1. Introduction

Shear waves, horizontal velocity fluctuations resulting from the instability of breaking wave–driven mean alongshore currents in the surf zone (Oltman-Shay et al. 1989; Bowen and Holman 1989), and surf beat, gravity waves believed to be excited by groups of shoaling sea swell waves (Munk 1949), both have periods of a few minutes. Here, three existing methods for estimating the magnitude of shear wave velocity fluctuations in the presence of gravity waves are compared.

Theory and observations suggest that shear waves have larger alongshore wavenumbers than gravity waves at a given frequency. Several methods estimate shear and gravity wave contributions to the velocity variance at each frequency using these different dispersion relations and the observed distribution of variance in alongshore wavenumber, determined from cross spectra between all pairs of current meters in an alongshore array. For example, Howd et al. (1991) use the iterative maximum likelihood estimator (IMLE; Pawka 1983) to calculate alongshore wavenumber k − frequency f spectra $E(k, f)$. At each frequency, the energy density associated with wavenumbers larger than the theoretical range for gravity waves is attributed to shear waves,

$$E_{sw}(f) = E(f) - \int_{k_{0-}(f)-\delta}^{k_{0+}(f)+\delta} E(k, f)\, dk, \qquad (1)$$

where $E_{sw}(f)$ is the energy density spectrum of shear waves and $E(f)$ is the energy density spectrum of all motions [i.e., shear plus gravity waves, equivalent to integration of $E(k, f)$ over all wavenumbers]. The border between gravity waves and shear waves in k–f space

* Woods Hole Oceanographic Institution Contribution Number 10368.

Corresponding author address: Dr. T. James Noyes, Scripps Institution of Oceanography, 9500 Gilman Drive, No. 209, La Jolla, CA 92093-0209.
E-mail: jnoyes@coast.ucsd.edu

is defined here by the dispersion curves of up- and downcoast propagating mode 0 edge waves, $k_{0\pm}(f)$, plus a small offset δ ($=0.0015$ m^{-1}) that accounts for their finite-wavenumber bandwidth. The linear shallow water equations are solved numerically to find $k_{0\pm}(f)$ for the measured bathymetry and mean alongshore current (Howd et al. 1992). Using the k–f spectrum of cross-shore u or alongshore v velocity in (1) yields the shear wave spectrum of cross-shore $E^u_{sw}(f)$ or alongshore $E^v_{sw}(f)$ velocity, respectively. The IMLE shear wave horizontal velocity variance $\langle q^2_{sw}\rangle$ is given by their sum integrated over the infragravity frequency band, defined here as $0.004 < f < 0.050$ Hz,

$$\langle q^2_{sw}\rangle = \int_{0.004\text{ Hz}}^{0.050\text{ Hz}} [E^u_{sw}(f) + E^v_{sw}(f)]\, df. \qquad (2)$$

A second method extracts direct estimates (DEs) of linear moments of the general form $\int G(k)E(k, f)\, dk$ from the observed cross spectra using a variational technique (Elgar et al. 1994). Here $E^u_{sw}(f)$ and $E^v_{sw}(f)$ are obtained from the u and v cross spectra, respectively, by setting $G(k) = 0$ inside the gravity wavenumber range $[k_{0-}(f) - \delta < k < k_{0+}(f) + \delta]$ and $G(k) = 1$ outside this range. The shear wave velocity variance estimate $\langle q^2_{sw}\rangle$ then follows from (2). The DE method makes no assumptions about the shape of $E(k, f)$ (IMLE exactly resolves plane waves in a noisy background), and optimizes the estimator fit to the observed cross spectra within a tolerance level based on data errors.

A third method [here referred to as the R method; Lippmann et al. (1999)] depends on the theoretically small contribution of shear waves to sea surface elevation fluctuations, and the theoretically equal partitioning of kinetic and potential energy in a broad spectrum of standing (edge or leaky) gravity waves. If only gravity waves are present, the ratio of kinetic to potential energy $R = (\langle q^2\rangle h)/(g\langle \eta^2\rangle) = 1$, where g is gravitational acceleration, h is the depth, and $\langle q^2\rangle$ and $\langle \eta^2\rangle$ are, respectively, the frequency-integrated, total (shear plus gravity wave) velocity and sea surface elevation variances,

$$\langle q^2\rangle = \int_{0.004\text{ Hz}}^{0.050\text{ Hz}} [E^u(f) + E^v(f)]\, df,$$

$$\langle \eta^2\rangle = \int_{0.004\text{ Hz}}^{0.050\text{ Hz}} E^\eta(f)\, df, \qquad (3)$$

where $E^u(f)$, $E^v(f)$, and $E^\eta(f)$ are the energy density spectra of cross- and alongshore velocity, and sea surface elevation, respectively. Shear waves are primarily horizontal motions, so they can contribute significantly to $\langle q^2\rangle$, but not to $\langle \eta^2\rangle$. Therefore, when both shear and gravity waves are present, $R > 1$, and the shear wave velocity variance is given by Lippmann et al. (1999),

$$\langle q^2_{sw}\rangle = \langle q^2\rangle - \frac{g\langle \eta^2\rangle}{h}. \qquad (4)$$

Unlike the IMLE and DE methods, which require array observations, the R method requires measurements of horizontal velocity and pressure fluctuations at only a single location. However, the R method estimates only the total shear wave variance $\langle q^2_{sw}\rangle$, providing no information about the distribution of shear waves in k–f space or the relative magnitudes of cross-shore and alongshore velocity fluctuations.

The observations and data analysis are described in section 2. In section 3, it is shown that when root-mean-square shear wave velocity fluctuations $\sqrt{\langle q^2_{sw}\rangle}$ are greater than a few centimeters per second, estimates of $\sqrt{\langle q^2_{sw}\rangle}$ from all three methods are similar and highly correlated, although R estimates are biased high. Estimator errors in conditions with low shear wave energy levels are discussed in section 4.

2. Observations and data analysis

Observations were obtained on a sandy beach near Duck, North Carolina, in the fall of 1997. Five, 200-m-long alongshore arrays of bidirectional current meters, sonar altimeters, and pressure sensors were deployed in depths from 1 to 5 m, approximately 50–250 m from the shoreline (Fig. 1), and were sampled at 2 Hz. About 2400 h of observations from each alongshore array were considered adequate for IMLE and DE analysis [at least five functioning current meters, including the instrument pair with the shortest (12 m) alongshore lag]. Bathymetry surveys, conducted a few times a week with an amphibious vehicle, were supplemented with sonar altimeter observations. For additional details and a description of conditions during the experiment, see Feddersen et al. (2000) and Elgar et al. (2001).

The pressure and velocity data were processed in 3-h segments that were quadratically detrended, and then divided into 448-s-long, demeaned, Hanning-windowed ensembles with 50% overlap. Results were not sensitive to detrending of the 448-s ensembles. Cross spectra and spectra with about 47 degrees of freedom and 0.0022-Hz frequency resolution were calculated for each 3-h period from the ensembles. For the low frequencies and shallow depths considered here, sea surface fluctuations were estimated by assuming that pressure is hydrostatic. For each 3-h data segment, IMLE and DE estimates of shear wave variance were calculated at each array, and R estimates were calculated at each collocated pressure–velocity sensor pair. Negative R estimates of shear wave variance [Eq. (4)] occurred infrequently (1% of all estimates) and were set equal to zero.

3. Comparison of IMLE, DE, and R methods

IMLE, DE, and R estimates for a representative 3-h-long run are shown in Fig. 2. Incident waves (significant

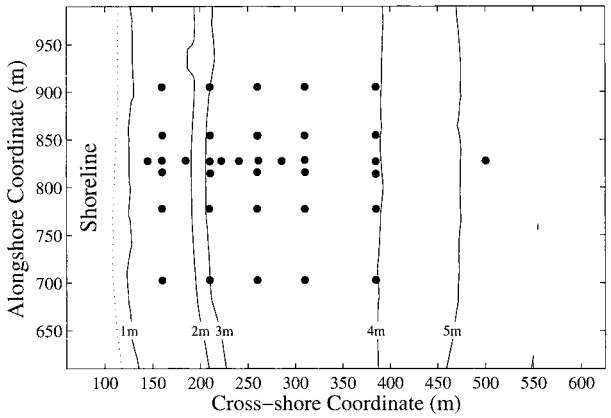

FIG. 1. Plan view of the sensor arrays. Symbols denote collocated pressure sensors, bidirectional electromagnetic current meters, and sonar altimeters (which measure the distance from a known vertical elevation to the evolving seafloor). Contours show the bathymetry on 24 Sep 1997, relative to mean sea level. The coordinate system of the Field Research Facility is used.

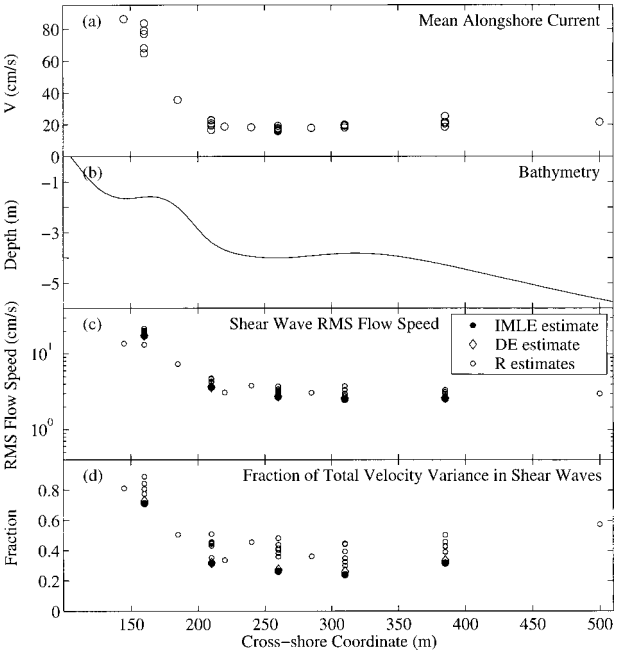

FIG. 2. (a) Mean alongshore current V, (b) bathymetry, (c) shear wave rms flow speed ($\sqrt{\langle q_{sw}^2 \rangle}$), and (d) fraction of the velocity variance in shear waves ($\langle q_{sw}^2 \rangle / \langle q^2 \rangle$) vs cross-shore coordinate on 24 Sep 1997. There is one R-method estimate for each collocated pressure gauge–current meter pair, and therefore there are multiple R estimates at the cross-shore locations of the five alongshore arrays. In (c) and (d), the IMLE and DE estimates are nearly identical.

wave height ~1 m) drove moderately strong mean alongshore currents V (Fig. 2a), reaching a maximum (~80 cm s^{-1}) near the crest of a shallow sandbar at x = 175 m (Fig. 2b). The DE and IMLE estimates of the root-mean-square, frequency-integrated, shear wave total horizontal velocity variance ($\sqrt{\langle q_{sw}^2 \rangle}$, referred to below as SW rms flow speed) are nearly identical at each alongshore array (Fig. 2c), as are their estimates of the fraction of the total velocity variance attributable to shear waves ($\langle q_{sw}^2 \rangle / \langle q^2 \rangle$, Fig. 2d). The R estimates from different pressure gauge–current meter pairs within the same alongshore array exhibit considerable variation, and are higher than DE and IMLE estimates. The difference between individual R estimates in the same array (for the same 3-h period) is nearly as large as the difference between the mean of the R estimates and the IMLE and DE estimates. The comparisons presented in the remainder of this paper (Figs. 4, 5, and 7) use the alongshore average of R estimates from a given array. All three methods show a large decrease in SW rms flow speed and SW fraction away from the region near the sandbar where the mean current is strong and highly sheared. Estimates of SW rms flow speed for the entire 4-month dataset show spatial variations similar to those of the 3-h run in Fig. 2.

Velocity energy density spectra $E(k, f)$ for this 3-h run, which were used to calculate the IMLE estimates in Fig. 2, show a characteristic shear wave ridge occupying the non–gravity wave region of k–f space (Oltman-Shay et al. 1989) both near the shoreline (Fig. 3a) where V and the cross-shore shear in V are strong, and at the most offshore array (Fig. 3b) where V is weak. The observed phase speed, determined from the slope of the shear wave ridge in k–f space, is larger at the shallowest array than at the most offshore array. This result is observed in many other cases, and will be discussed in a subsequent publication. IMLE and DE estimates of the energy density spectra of shear wave horizontal velocity [$E_{sw}^u(f) + E_{sw}^v(f)$] are nearly identical (Fig. 3, right panels). At the shallow array, shear waves contribute more than 50% of the total (gravity plus shear wave) horizontal velocity variance at all frequencies less than ~0.04 Hz. At the deep array, where both the total and shear wave energy levels are an order of magnitude lower than at the shallow array, shear waves are dominant only below ~0.01 Hz.

Model simulations show that IMLE estimates may be affected by aliasing of energy from wavenumbers with magnitudes greater than the Nyquist wavenumber (about 0.04 m^{-1}, corresponding to the minimum alongshore array lag of 12 m). For example, in the observations shown in Fig. 3, the shear wave ridges extend to −0.04 m^{-1} and may reappear at positive wavenumbers owing to aliasing (e.g., Fig. 3a at 0.03 Hz and Fig. 3b at 0.01 Hz). However, shear wave energy levels are relatively low at the possibly aliased frequencies in these data.

Correlations between IMLE, DE, and R estimates of SW rms flow speed for the entire dataset are high, above 0.96 (Fig. 4a). On average, DE SW rms flow speed estimates are slightly higher (less than 10% at all SW rms flow speeds; Fig. 4b) than IMLE estimates, and both the bias and standard deviations of DE relative to IMLE decrease with increasing SW rms flow speed. The mean (e.g., alongshore averaged) R estimates show higher bias (between 20% and 60%) and larger standard

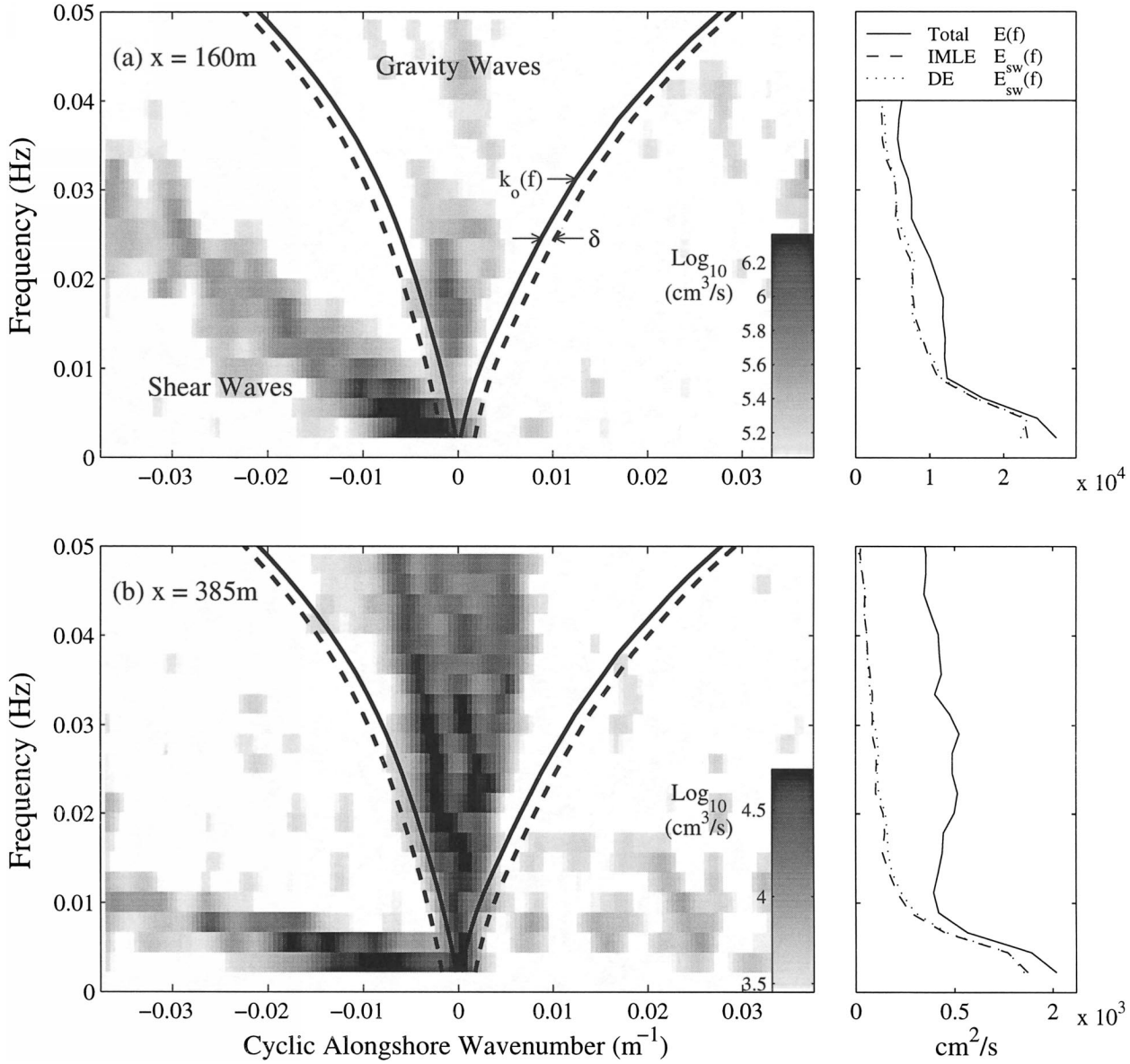

FIG. 3. (left panels) IMLE alongshore wavenumber–frequency spectra of horizontal velocity energy density $E^u(k, f) + E^v(k, f)$ estimated from alongshore arrays at cross-shore positions (a) $x = 160$ m and (b) $x = 385$ m (the shallowest and deepest arrays) on 24 Sep 1997. A different grayscale is given in each panel. Cyclic alongshore wavenumber is the reciprocal of the wavelength. Gravity waves occur in the region of k–f space bounded by the mode 0 edge wave dispersion curves $k_0(f)$ (solid curves) plus a small offset δ ($=0.0015$ m^{-1}) (dashed curves). (right panels) Total (shear plus gravity waves, solid curve) energy density spectrum $E(f)$, and IMLE (dashed curve) and DE (dotted curve) shear wave energy density spectra $E_{sw}(f)$. IMLE and DE $E_{sw}(f)$ are nearly identical. Note that the scales for $E(f)$ in (a) and (b) differ by a factor of about 30.

deviations relative to IMLE, with the largest bias and scatter at low SW rms flow speeds. Individual R estimates (not shown) display about twice as much scatter as alongshore-averaged R estimates (Fig. 4). The DE and IMLE estimates of the SW fraction are nearly identical (Fig. 5). Mean R estimates of the SW fraction are on average 0.15 higher than the IMLE estimates, with considerable scatter.

Simulations with known mixes of shear and gravity waves suggest that IMLE and DE estimator errors, owing to array geometry and statistical fluctuations in the cross spectra, are small unless shear wave energy levels are low (see the appendix). For true (e.g., simulated) SW rms flow speeds greater than 2 cm s^{-1}, the mean bias of IMLE and DE estimates of SW rms flow speed (relative to the true value) is less than 10% (Fig. A1a). When shear waves contain more than 30% of the total variance, the mean bias of IMLE and DE estimates of the SW fraction is less than 15% of the true fraction (Fig. A1b). The bias in IMLE and DE estimates is largest

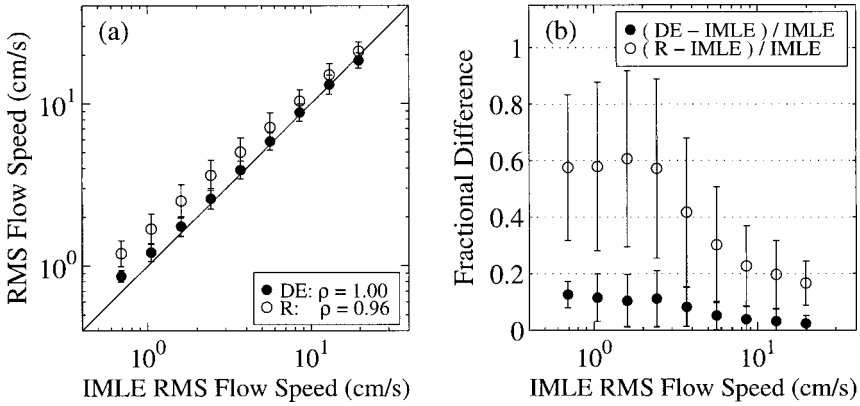

FIG. 4. (a) The DE (solid circles) and R (open circles) estimates of shear wave rms flow speed ($\sqrt{\langle q_{sw}^2 \rangle}$) vs IMLE estimates of shear wave rms flow speed. The means (circles) and standard deviations (vertical bars) are based on the estimates in each bin. The correlations ρ of the unbinned data (3684 estimates) are given in the legend. (b) The fractional difference between IMLE rms flow speed and DE and R rms flow speed estimates vs IMLE rms flow speed.

at the lowest values of SW rms flow speed and SW fraction (which tend to occur together).

4. Discussion

All three methods estimate that shear waves contribute at least 10%–20% of the total infragravity velocity variance, even when the mean alongshore current V is weak and likely stable (i.e., shear waves are absent). For example, when V is less than 10 cm s^{-1} at all current meters, the average R value is 1.5, and an implausibly large 33% of the infragravity velocity variance is ascribed to shear waves. Including non–gravity wave sea surface elevation variance $\langle \eta_{sw}^2 \rangle$ in $\langle \eta^2 \rangle$ will bias R estimates low [Eq. (4)], rather than high as observed. However, estimates of $\langle \eta_{sw}^2 \rangle / \langle \eta^2 \rangle$, with $\langle \eta_{sw}^2 \rangle$ derived from integration of IMLE pressure $E(k, f)$ spectra over non–gravity wavenumbers, are on average less than 0.05 for all SW rms flow speeds, too small to affect R estimates significantly. When shear wave energy is low, a significant fraction of the IMLE and DE estimates of $\langle q_{sw}^2 \rangle$ comes from energy that is broadly distributed in k–f space, rather than concentrated on a shear wave ridge (e.g., about 1/3 of the DE and IMLE estimates of $\langle q_{sw}^2 \rangle$ in Fig. 3b is at $f > 0.02$ Hz). Simulations show that for true SW fractions less than 10%, bias errors in SW fraction as large as 80% (Fig. A1b) result from spectral leakage from the much more energetic gravity waves (IMLE and DE methods). Thus, when V and shear wave levels are small, all three estimates of shear wave velocity variance are inaccurate.

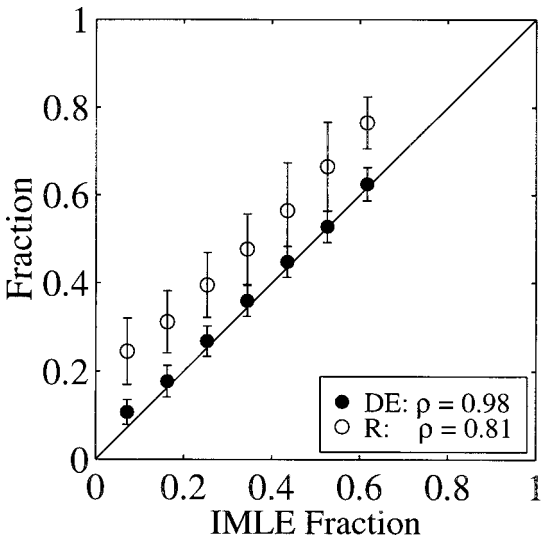

FIG. 5. The DE (solid circles) and R (open circles) estimates of the fraction of the total velocity variance in shear waves ($\langle q_{sw}^2 \rangle / \langle q^2 \rangle$) vs IMLE estimates of the fraction of the total velocity variance in shear waves. The means (circles) and standard deviations (vertical bars) are based on the estimates in each bin. The correlations ρ of the unbinned data (3684 estimates) are given in the legend.

Observations (Oltman-Shay et al. 1989), linear stability theory (Bowen and Holman 1989), and numerical simulations (Allen et al. 1996) suggest that shear waves are most energetic at the lowest infragravity frequencies and propagate preferentially in the direction of the mean alongshore current. Thus, high asymmetry between upcoast and downcoast propagation of shear wave energy,

$$\text{SW asymmetry} = \frac{\langle q_{sw}^2 \rangle_{up} - \langle q_{sw}^2 \rangle_{down}}{\langle q_{sw}^2 \rangle_{up} + \langle q_{sw}^2 \rangle_{down}}, \qquad (5)$$

in the frequency band 0.004–0.010 Hz is consistent with the presence of energetic shear waves, whereas low asymmetry suggests shear waves may not be present. The SW asymmetry (estimated with IMLE) is aligned with the mean alongshore current V at each location, and becomes larger as V increases (Fig. 6). The SW asymmetry also increases with increasing SW rms flow speed (Fig. 7). Upcoast propagating energy exceeds downcoast (or vice versa) by more than a factor of 2

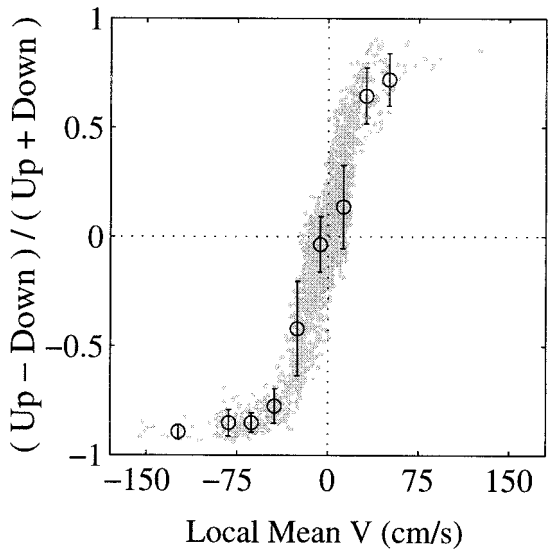

FIG. 6. IMLE-estimated asymmetry in the upcoast–downcoast propagation of shear wave energy [Eq. (5)] in the frequency band 0.004–0.010 Hz vs the mean alongshore current at the same cross-shore shore location. Each gray dot is an individual (e.g., unbinned) 3-h estimate. The means (circles) and standard deviations (vertical bars) are based on the estimates in each bin.

(SW asymmetry > 0.33) for V greater than 25 cm s^{-1}, and for IMLE (mean R) SW rms flow speeds greater than $\sim$4 (6) cm s^{-1}. The low SW asymmetries associated with the weakest V (Fig. 6) and lowest SW rms flow speeds (Fig. 7) suggest that shear waves are not responsible for a significant portion of the variance in these cases, and that the estimates of SW rms flow speed are inaccurate.

Flowmeter noise may be significant when shear wave energy is low. The R method ascribes any noise in the observed horizontal velocity variance $\langle q^2 \rangle$ to shear waves [Eq. (4)]), but broad-banded (in wavenumber) noise contributes less to IMLE and DE shear wave estimates, because the noise variance is split between shear and gravity waves. Velocity fluctuations not associated with gravity or shear waves [e.g., instabilities of the undertow; Li and Dalrymple (1998)] also may degrade all three estimates. The relative importance of different error sources (e.g., spectral leakage from gravity waves, flowmeter noise, other instabilities) is unknown.

5. Conclusions

Three methods are shown to produce similar estimates of shear wave variance. Iterated maximum likelihood (IMLE, Howd et al. 1991) and direct (DE, Elgar et al. 1994) estimates of SW rms flow speed are both obtained from arrays of current meters, and differ by less that 10% when shear wave velocity fluctuations are greater than a few centimeters per second. Estimates from individual collocated pressure gauge–current meter pairs [R method; Lippmann et al. (1999)] are similar to those from arrays, but are biased high, typically attributing about 15% more of the horizontal velocity variance to shear waves than is attributed by IMLE or DE estimates. The difference between individual R estimates in the same array (for the same 3-h period) can be as large as the difference between the mean of the R estimates and the IMLE and DE estimates. When shear wave velocity fluctuations are less than a few centimeters per second, shear wave variance estimates from all three methods are noisy and biased high. Although the estimates differ in detail, the high correlations (>0.96 for SW rms flow speed) between them lend support to their underlying assumptions.

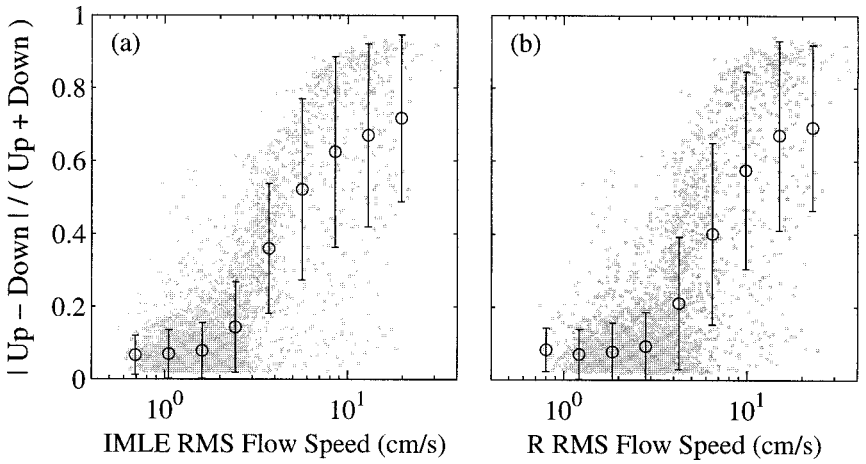

FIG. 7. The magnitude of the IMLE-estimated asymmetry in the upcoast–downcoast propagation of shear wave energy [Eq. (5)] in the frequency band 0.004–0.010 Hz vs (a) IMLE and (b) R estimates of shear wave rms flow speed ($\sqrt{\langle q_{sw}^2 \rangle}$). Each gray dot is an individual (e.g., unbinned) 3-h estimate. The means (circles) and standard deviations (vertical bars) are based on the estimates in each bin.

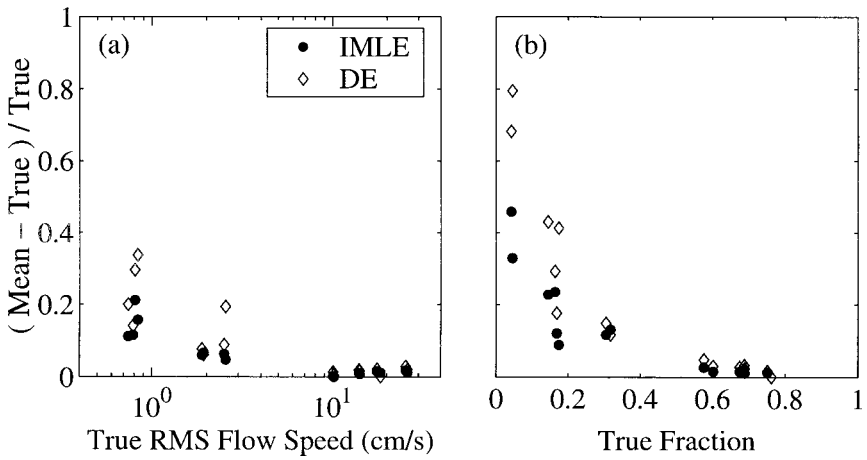

FIG. A1. The average bias of IMLE and DE estimates (normalized by the true values) of (a) shear wave rms flow speed ($\sqrt{\langle q_{sw}^2 \rangle}$) and (b) the fraction of the total velocity variance in shear waves ($\langle q_{sw}^2 \rangle / \langle q^2 \rangle$) vs the true values.

Acknowledgments. This research was supported by the Office of Naval Research Coastal Dynamics and the National Ocean Partnership Program. Staff from the Center for Coastal Studies, Scripps Institution of Oceanography, and from the U.S. Army Corps of Engineers Field Research Facility, Duck, North Carolina, provided excellent logistic support.

APPENDIX

Numerical Simulations

Simulations were used to assess the effects of array geometry and of statistical fluctuations in cross spectra on the accuracy of the IMLE and DE estimates. The simulations did not address the underlying assumption that shear wave energy occurs only at wavenumbers larger than gravity wave wavenumbers, nor the accuracy of the *R* method. A subset of the observed IMLE alongshore wavenumber–frequency spectra $E(k, f)$ of cross- and alongshore velocity components that span the range of observed shear wave variance were selected for use as target test spectra. In additional simulations, the total variance, mean wavenumber, and rms wavenumber were calculated for each frequency band in each of three domains (gravity waves, and upcoast and downcoast propagating shear waves) using observed IMLE spectra. These quantities were then used to define the amplitude, peak wavenumber, and width of three Gaussian distributions in each frequency band of synthetic test spectra. Simulations with observed and synthetic (Gaussian shaped) spectra yield similar results.

Test $E(k, f)$ spectra were Fourier transformed into cross spectra between pairs of sensors in an alongshore array. Random, Gaussian statistical fluctuations consistent with 47 degrees of freedom were added to the test cross spectra in each frequency band, and the IMLE and DE methods were applied to 1000 such realizations of every k–f test spectrum. The means of the 1000 IMLE and DE estimates of SW rms flow speed and SW fraction relative to the true values are shown in Fig. A1. IMLE and DE estimate errors have similar statistics. The estimator bias is a smaller fraction of the true value as SW rms flow speed and SW fraction increase, and is less than 10% except at the lowest levels of SW rms flow speed (less than 2 cm s^{-1}) and SW fraction (less than 0.3). The error standard deviations (not shown) remain less than 5% for SW rms flow speeds greater than 2 cm s^{-1} and SW fractions greater than 0.3, but are up to 40% of the means at lower SW rms flow speeds and SW fractions. The increased variability and bias in simulations with low shear wave energies is caused by leakage from the more energetic gravity waves.

REFERENCES

Allen, J. S., P. A. Newberger, and R. A. Holman, 1996: Nonlinear shear instabilities of alongshore currents on plane beaches. *J. Fluid Mech.,* **310,** 181–213.

Bowen, A. J., and R. A. Holman, 1989: Shear instabilities of the mean longshore current, 1, Theory. *J. Geophys. Res.,* **94,** 18 023–18 030.

Elgar, S., T. H. C. Herbers, and R. T. Guza, 1994: Reflection of ocean surface gravity waves from a natural beach. *J. Phys. Oceanogr.,* **24,** 1503–1511.

——, R. T. Guza, W. C. O'Reilly, B. Raubenheimer, and T. H. C. Herbers, 2001: Wave energy and direction observed near a pier. *J. Waterway, Port, Coastal Ocean Eng.,* **127,** 2–6.

Feddersen, F., R. T. Guza, S. Elgar, and T. H. C. Herbers, 2000: Velocity moments in alongshore bottom stress parameterizations. *J. Geophys. Res.,* **105,** 8673–8686.

Howd, P. A., J. Oltman-Shay, and R. A. Holman, 1991: Wave variance partitioning in the trough of a barred beach. *J. Geophys. Res.,* **96,** 12 781–12 795.

——, A. J. Bowen, and R. A. Holman, 1992: Edge waves in the presence of strong longshore currents. *J. Geophys. Res.,* **97,** 11 357–11 371.

Li, L., and R. A. Dalrymple, 1998: Instabilities of the undertow. *J. Fluid Mech.,* **369,** 175–190.

Lippmann, T. C., T. H. C. Herbers, and E. B. Thornton, 1999: Gravity and shear wave contributions to nearshore infragravity motions. *J. Phys. Oceanogr.*, **29,** 231–239.

Munk, W. H., 1949: Surf beats. *Trans. Amer. Geophys. Union,* **30,** 849–854.

Oltman-Shay, J., P. Howd, and W. Birkemeier, 1989: Shear instabilities of the mean longshore current, 2, Field observations. *J. Geophys. Res.,* **94,** 18 031–18 042.

Pawka, S., 1983: Island shadows in wave directional spectra. *J. Geophys. Res.,* **88,** 2579–2591.